NANO LETTERS

Letter

pubs.acs.org/NanoLett

Near-Field Energy Extraction with Hyperbolic Metamaterials

Jiawei Shi, Baoan Liu, Pengfei Li, Li Yen Ng, and Sheng Shen*

Department of Mechanical Engineering, Carnegie Mellon University, Pittsburgh, Pennsylvania 15213, United States

Supporting Information

ABSTRACT: Although blackbody radiation described by Planck's law is commonly regarded as the maximum of thermal radiation, thermal energy transfer in the near-field can exceed the blackbody limit due to the contribution from evanescent waves. Here, we demonstrate experimentally a broadband thermal energy extraction device based on hyperbolic metamaterials that can significantly enhance near-field thermal energy transfer. The thermal extractor made from hyperbolic metamaterials does not absorb or emit any radiation but serves as a transparent pipe guiding the radiative energy from the emitter. At the same gap between an emitter and an absorber, we observe that near-field thermal energy transfer with thermal extraction can be enhanced by around 1 order of magnitude, compared to the case without thermal extraction. The novel thermal extraction scheme has important practical implications in a variety of technologies, e.g., thermophotovoltaic energy conversion, radiative cooling, thermal infrared imaging, and heat assisted magnetic recording.

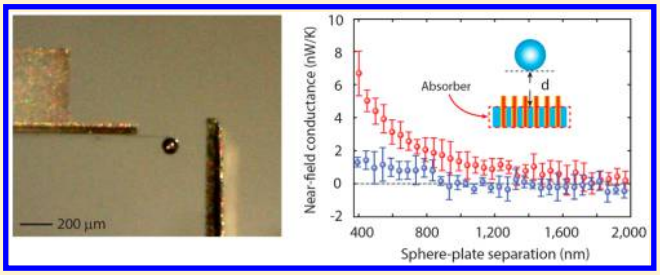

KEYWORDS: *Near field, energy transfer, hyperbolic metamaterials*

Control of thermal emission is important in a broad range of applications: e.g., thermal management,[1] energy conversion,[2] thermal barriers,[3] and thermal signature control.[4] Blackbody radiation described by the well-known Planck's law[5] dictates the maximum of thermal radiation in the far-field. To enhance the far-field thermal radiation from a blackbody emitter, a "thermal extraction" scheme has recently been developed by optically contacting the emitter with a passive extraction device.[6] Although the extraction device itself is transparent for thermal radiation, its internal density of states is higher than vacuum and therefore enables more emission channels by extracting evanescent electromagnetic waves with lateral wave vector K in the range of $k_0 < K < n_e k_0$, where k_0 is the wave vector in vacuum and n_e is the refractive index of the extraction device. The performance of such far-field extraction devices is limited by n_e^2 times of the blackbody radiation limit. In contrast, near-field thermal extraction, where the characteristic length scale is smaller than the wavelength of thermal radiation,[7] can potentially overcome this limitation by extracting a full range of evanescent waves. In this Letter, we demonstrate broadband near-field thermal extraction based on hyperbolic metamaterials (HMs), which can significantly enhance near-field energy transfer by extracting evanescent waves with arbitrarily large lateral wave vectors. The near-field thermal extraction has important practical implications in areas, such as thermophotovoltaic energy conversion,[8] radiative cooling,[9] thermal infrared imaging,[10] and heat-assisted magnetic recording.[11]

As a special class of indefinite media, HMs with the principal components of the permittivity tensor ϵ having opposite signs have attracted significant interest because of their unique properties, such as negative refraction and subwavelength imaging.[12] The dispersion relation of HMs generally satisfies a hyperbolic function (red curves in Figure 1a):

$$\frac{k_z^2}{\epsilon_{x,y}} - \frac{K^2}{|\epsilon_z|} = k_0^2 \tag{1}$$

where ϵ_z is the vertical component ($\epsilon_z < 0$), $\epsilon_{x,y}$ is the lateral component ($\epsilon_{x,y} > 0$) with the materials assumed to be uniaxial (i.e., $\epsilon_x = \epsilon_y = \epsilon_{x,y}$), and k_z and K are the vertical and lateral components of the wavevector, respectively. If a point source is located near a HM, its emitted evanescent waves in vacuum (wave vector $k = (k_z^2 + K^2)^{1/2} > k_0$) can excite propagating modes in the HM, leading to enhanced photon local density of states (PLDOS). To illustrate near-field thermal extraction, we consider radiative heat transfer between an emitter and an absorber, where a lossless HM (i.e., a real permittivity tensor ϵ) is placed between the emitter and the absorber and is in contact with the emitter as a thermal extraction device. If the gap between the emitter and the absorber is large compared with the wavelength of thermal radiation, evanescent waves from the emitter cannot directly contribute to heat transfer because of their exponential attenuation across the gap. However, according to eq 1, these evanescent waves can be converted into propagating waves in the HM and thus transfer energy from the emitter to the absorber. In comparison with the extraction device for far-field emission,[6] an ideal HM extractor could introduce an unlimited number of energy transfer channels between the emitter and the absorber.

Received: November 11, 2014
Revised: January 23, 2015
Published: January 26, 2015

DOI: 10.1021/nl504332t
Nano Lett. 2015, 15, 1217−1221

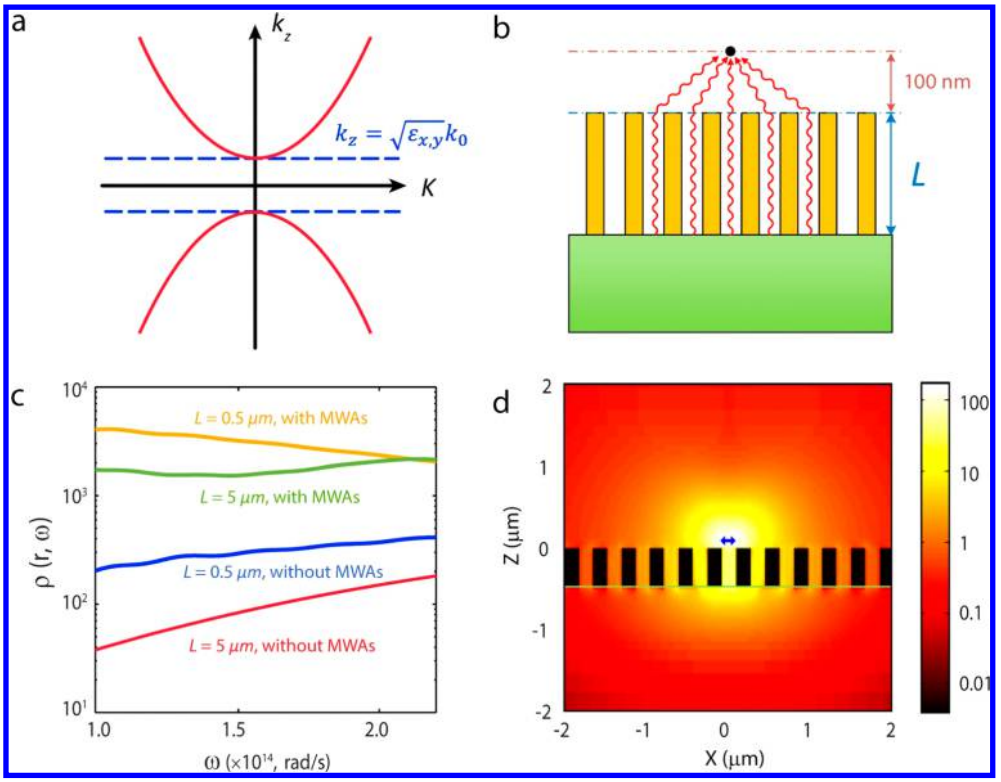

Figure 1. HMs mediated near-field thermal extraction. (a) Dispersion relation of typical HMs (red curves) and MWAs (blue dashed lines). (b) Schematic of the MWA-based near-field thermal extractor. (c) Calculated PLDOS at 100 nm above MWAs for different lengths L = 500 nm and L = 5 μm with/without the MWAs. (d) Electric field intensity excited by a dipole located at 100 nm above the 500 nm thick slab of MWAs.

A number of structures, such as alternating metal−dielectric layers and metal wire arrays (MWAs), have been proposed to realize HMs. In the infrared regime, metals behave like perfect electric conductors that barely emit or absorb light. Metamaterials made from MWAs are extremely low-loss and can maintain the hyperbolic dispersion in a broad frequency band.[13] Particularly, MWAs were demonstrated to be broadband infrared and terahertz waveguides with a dispersion relation, $k_z = (\epsilon_{x,y})^{1/2} k_0$, which corresponds to a HM with $\epsilon_z = \infty$, reducing the hyperbolic function to two flat lines (blue dashed lines in Figure 1a).[14] As a result, MWAs perform as lossless waveguides that can duplicate the exact field profiles at one end and transfer them to the other end. To quantitatively evaluate the performance of MWAs as a near-field thermal extractor, we calculate the PLDOS near a slab made from MWAs. For a system at thermal equilibrium, the general formulation of PLDOS, $\rho(r,\omega)$, is expressed by

$$\rho(r, \omega) = \langle U(r, \omega) \rangle / \left(\frac{\hbar\omega}{\exp(\hbar\omega/k_B T) - 1} \right) = \frac{\omega}{\pi c^2} \mathrm{Im}\, Tr[\overleftrightarrow{G}^{E}(r, r, \omega) + \overleftrightarrow{G}^{H}(r, r, \omega)], \quad (2)$$

where $\langle U \rangle$ is the local energy density of thermal radiation and G^E and G^H are the electric and magnetic dyadic Green functions of an inhomogeneous system, respectively.[15] Here, $\rho(r,\omega)$ can be understood as the average number of thermally emitted photons at location r, which includes contributions from both propagating and evanescent waves.

As one example, a HM slab composed of MWAs is in close contact with an emitter having a refractive index n = 1.5 + 1.5i (Figure 1b). The period and the radius of MWAs are set to be 350 and 100 nm, respectively, which ensures a hyperbolic dispersion of the MWAs in the infrared range. In Figure 1c, the calculated PLDOS at a distance of 100 nm above the HM slab can be enhanced by 1 order of magnitude, compared with the PLDOS at the same location without the HM slab. Moreover, the 5 μm thick slab has similar PLDOS enhancement with the 500 nm thick slab. This is because the waveguiding properties or the HM characteristics of MWAs are almost independent of the wire length, as long as the period of the wires is much smaller than the lateral wavelength of incident photons. The HM modes in MWAs are extremely low-loss because electromagnetic energy is highly concentrated on metal wire surfaces with little penetration. The decay length of MWAs, for example, nickel wire arrays, is estimated to be ∼100 μm at the wavelength of 10 μm. Figure 1d shows the electric field profile excited by a dipole located at a 100 nm distance above the 500 nm thick slab. The uniform field distribution along the wires further confirms the waveguiding effect of MWAs.

We demonstrate near-field thermal extraction by measuring the radiative heat transfer between a microsphere and a substrate at nanoscale gaps (Figures 2a and b). To prepare the near-field thermal probe, a 100 μm diameter SiO_2 (glass) microsphere is attached to the tip of a bimaterial (SiN_X/gold) atomic force microscope (AFM) cantilever, which can resolve heat power as small as 0.1 nW because of the bimetallic effect.[16,17] A laser beam is used to measure the deflection of the cantilever and heat the microsphere to ∼50 °C, whereas the sample substrate is maintained at ambient temperature. When the sphere approaches the substrate, the heat flow radiated from the microsphere to the substrate greatly increases due to near-field heat transfer.[18,19] The resulting temperature change of the sphere causes the bending of the cantilever that is further

DOI: 10.1021/nl504332t
Nano Lett. 2015, 15, 1217−1221

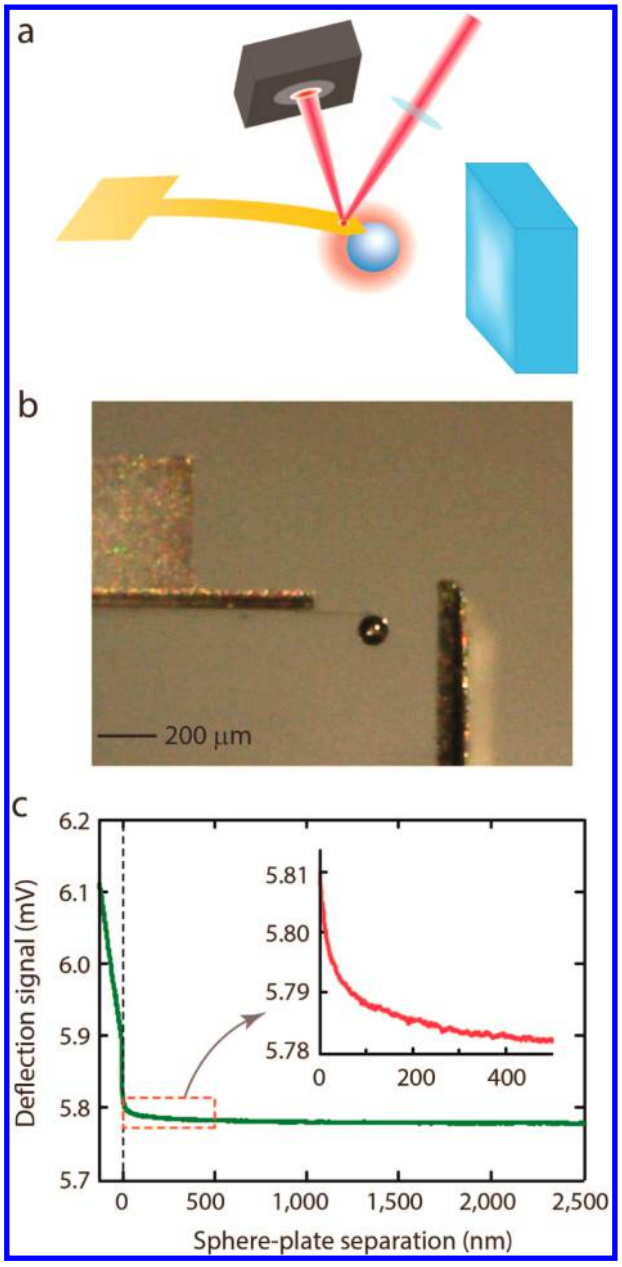

Figure 2. Experimental setup for near-field thermal measurements. (a) Schematic of the experiment setup that shows the relative position between the optical deflection system and the sample. (b) Optical image of the setup. (c) Typical cantilever deflection signals when the sphere approaches the substrate. The contact point between the sphere and the plate is marked by the vertical dashed black line. Inset: Deflection signals close to the contact point.

monitored and measured using an optical deflection system. In our experiment, the gap between the sphere and the substrate is continuously reduced at a speed of 20 nm/s in order to minimize the influence of thermal drift of the AFM cantilever. As shown in Figure 2c inset, the deflection signal of the cantilever, which also represents the near-field heat transfer signal, increases as the gap decreases with time. The sharp change in the slope of cantilever deflection signals indicates the mechanical contact between the sphere and the substrate (Figure 2c), thereby providing a reference to precisely determine the substrate-sphere separation.

To fabricate the MWAs based HMs, we employ anodic aluminum oxide (AAO) nanoporous templates to grow vertically aligned metal nanowires via electrochemical deposition.[20−22] Figures 3a and b show nickel nanowire arrays

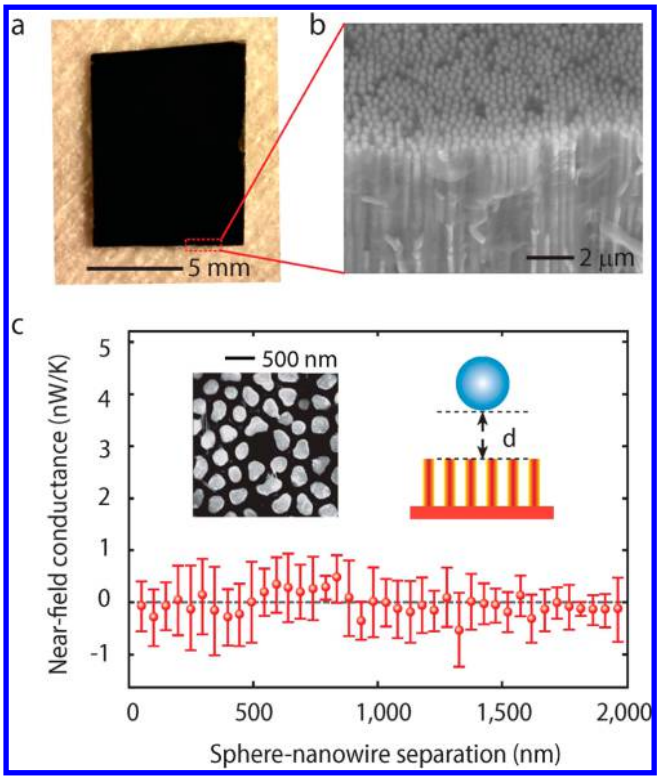

Figure 3. Fabrication of a HM composed of MWAs and its application as low-loss waveguides. (a) Optical image of the polished nickel nanowire−AAO composite. (b) SEM image of the side view of the polished sample shown in a. (c) Near-field heat transfer between a SiO_2 sphere and free-standing nanowire arrays as a function of nanowire−sphere separation. The dashed line indicating zero near-field conductance is drawn for eye guidance. The upper left inset is the SEM image of the top view of free-standing nanowires, where the nanowires are well-separated from each other after supercritical drying.

embedded in an AAO template. To prove that MWAs do not participate in heat transfer as a passive waveguide, we measure the near-field radiative heat flux between the SiO_2 microsphere and bare nickel nanowire arrays in vacuum supported on a ∼30 μm thick nickel film. The length and the diameter of the nickel nanowires are ∼10 μm and ∼300 nm, respectively. The separation between the nanowires is ∼100 nm on average (Figure 3c, upper left inset). The temperature difference between the SiO_2 sphere and the nickel nanowires was calibrated to be 29 K. As a polar dielectric, SiO_2 supports resonant surface phonon polariton modes and serves as a super-Planckian near-field absorber/emitter (with a very large PLDOS close to its surface).[18] The nickel film beneath the nanowires performs as a mirror - an extremely inefficient thermal emitter/absorber.

It has been demonstrated that the near-field heat transfer between a SiO_2 sphere and a metal surface is almost zero.[18] If substantial heat transfer occurs between the SiO_2 sphere and the nickel nanowires, it must be attributed to the contribution from the nickel nanowires rather than the 30 μm thick nickel film. However, there is no obvious heat transfer observed in Figure 3c, where the measured near-field thermal conductance

DOI: 10.1021/nl504332t
Nano Lett. 2015, 15, 1217−1221

is plotted as a function of the separation between the nanowires and the sphere. This is because the nanowires are low-loss for thermal radiation, and therefore the propagating waves along the 10 μm long nanowires have negligible dissipation. On the other hand, when the nondecaying propagating waves reach the highly reflective nickel film at the end of the nanowires, they will be almost totally reflected. As a result, the measured near-field heat transfer is close to zero, even at a sphere−nanowire separation smaller than 50 nm. Our measurements clearly demonstrate that nickel nanowire arrays can work as a passive loss-less waveguide for thermal radiation.

We experimentally investigate near-field thermal extraction by connecting MWAs with a lossy thermal emitter/absorber instead of a metal mirror in the above case. The sample is prepared by partially etching the AAO template in a NaOH solution. In Figure 4a and b, the nickel nanowire arrays protrude ~400 nm from the AAO template after etching. The rest portion of the nanowires together with the alumina template (dashed red box in Figure 4c, inset) serve as a high-performance thermal absorber. The absorptivity of the nickel nanowire/alumina composite is mainly attributed to two effects: (1) the intrinsic surface phonon-polariton resonance of alumina leads to the strong enhancement of PLDOS at the resonance frequencies; (2) the embedded nickel nanowires provide broadband hyperbolic modes, which in general enhance the PLDOS at the nonresonating frequencies (see Supporting Information). To demonstrate near-field thermal extraction effect, we measure the near-field heat transfer with/without the protruded nickel nanowires as a thermal extractor. In Figure 4c, where near-field thermal conductance is plotted as a function of the gap d between the SiO_2 sphere and the AAO template (substrate) (Figure 4c, upper right inset), the HM thermal extractor (i.e., ~400 nm long nanowires) can dramatically enhance near-field heat transfer. At the smallest separation (~10 nm) between the sphere and the nanowires that corresponds to $d \sim 400$ nm, the measured thermal conductance with the protruded nanowires is ~7 nW/K, which is around 1 order of magnitude larger than the case without the protruded nanowires (~1 nW/K). This result demonstrates the excellent near-field thermal extraction performance of MWAs. It is worth to note that in order to demonstrate the near-field thermal extraction effect of MWAs, the near-field emitters and absorbers can be arbitrarily chosen. The thermal absorber made from the nanowire/alumina composite in this work only serves as one example without losing generality.

Here, we want to emphasize that near-field thermal extraction of MWAs is independent of the material properties of emitters/absorbers. For any thermal emitters/absorbers, such as a lossy AAO template or a SiO_2 sphere in this work, they all support thermally excited evanescent waves. The evanescent modes can be surface polariton modes for polar dielectrics or metals or nonresonant evanescent modes for other materials. When the emitter and the absorber are separated by a large gap compared to the wavelength of thermal radiation, all of these evanescent modes exponentially decay from surface and have no contribution to heat transfer. However, if a HM (e.g., MWAs) optically contacted with the emitter and was placed between the emitter and the absorber, the evanescent modes from the emitter can be converted into the propagating modes in the HM, and then transfer energy to the absorber via the near-field coupling between the HM and the absorber. Hence, radiative heat transfer can be greatly enhanced by the extracted evanescent modes. Although we only

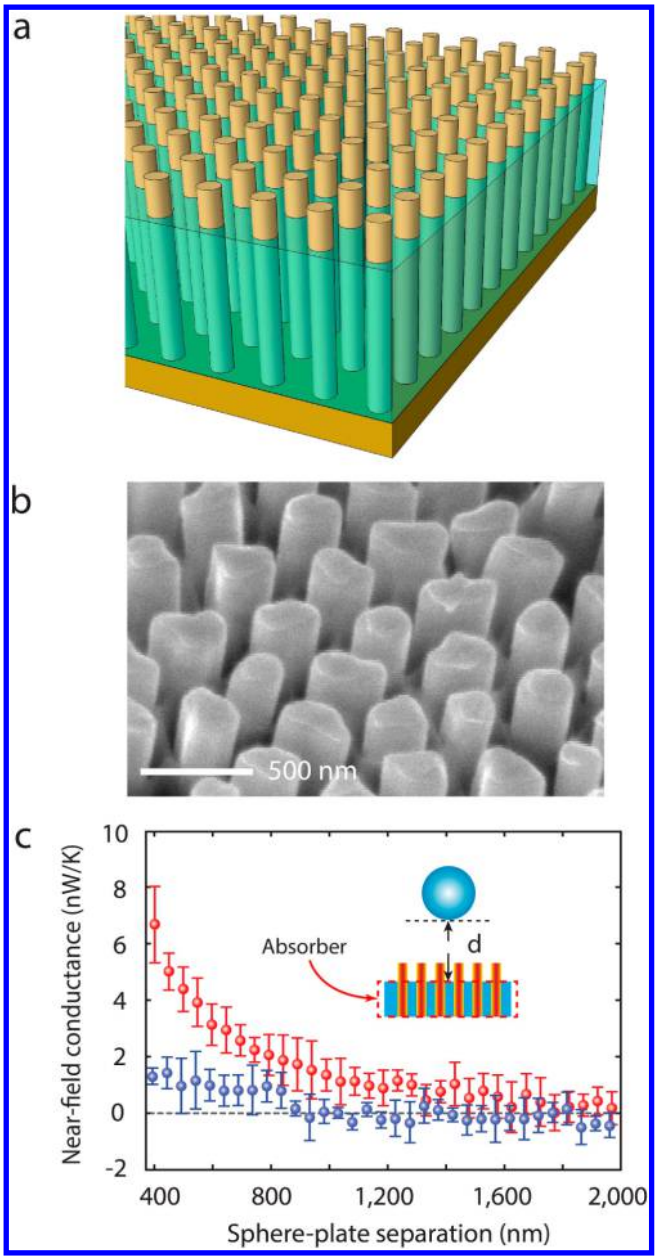

Figure 4. Experimental demonstration of near-field thermal extraction. (a) Schematic and (b) SEM image of partially released nickel nanowire arrays. The protruded nanowires are measured to be ~400 nm from the AAO template. (c) Near-field heat transfer as a function of the gap between the sphere and the AAO template with (red dots) and without (blue dots) the protruded nanowires. The dashed line indicating zero near-field conductance is drawn for eye guidance. The separation between the sphere and the substrate (AAO template) ends at ~400 nm because of the protruded nanowires.

demonstrate near-field thermal extraction using ~400 nm long nanowires in this work, thermal extractors made from MWAs are expected to maintain good extraction performance for much longer nanowires (e.g., 10 μm long nanowires) as well because of the low-loss waveguide modes in MWAs (Figure 1c).

In summary, we experimentally demonstrate a HMs mediated energy extraction device that can significantly enhance near-field heat transfer by about 1 order of magnitude. In particular, the HMs made from MWAs are low-loss for thermal radiation and perform as passive and transparent pipes guiding radiative energy. Our work opens up a myriad of new

DOI: 10.1021/nl504332t
Nano Lett. 2015, 15, 1217−1221

thermal applications based on metamaterials. The high thermal extraction with HMs can be exploited to develop a variety of technologies ranging from thermophotovoltaic energy conversion to thermal imaging.

Methods. *Sample Fabrication.* A thin layer of nickel (~100 nm in thickness) is first sputtered on one side of the AAO template as a seed layer for electroplating. When nickel nanowires grow out of the AAO template, they will coalescence into a thin metal film. Chemical mechanical planarization (CMP) is then applied to obtain a flat and smooth surface for subsequent near-field measurements.[23] The roughness of the polished surface can normally reach ~5 nm after planarization, thus ensuring the uniform height of nickel nanowires. The nanowire arrays can be completely released by dissolving the AAO template in a NaOH aqueous solution. To prevent the released nanowires from collapsing into bundles due to surface tension, supercritical drying is used to remove liquid.

Near-Field Thermal Measurement. Our experimental details have been described in previous publications.[17,18,24] In the experiment, the cantilever with the microsphere is oriented perpendicularly to the substrate to reduce the bending caused by Casimir and electrostatic forces. The entire setup is placed on a mechanical vibration isolator, and the measurement is conducted under a vacuum level of $\sim 1 \times 10^{-6}$ Torr in order to eliminate the air heat conduction between the sphere and the substrate. The surface roughness of the microsphere is measured to be ~4 nm by an AFM.[24] The substrate is rigidly fixed onto a three-dimensional piezoelectric translation stage with a step resolution of 1 nm. Most of the laser power absorbed by the cantilever tip is transferred along the cantilever to its supporting base, but a small amount (<0.5%) of absorbed heat is radiated from the cantilever and the sphere to the surrounding (including the substrate). The measured cantilever deflection signal in Figure 2c is linearly proportional to heat transfer. By calibrating the cantilever, its deflection signal can be converted into the heat transfer between the sphere and the substrate.

■ ASSOCIATED CONTENT

Supporting Information

Numerical calculation of PLDOS, growth of metal nanowires via electrochemical deposition, and chemical mechanical planarization. This material is available free of charge via the Internet at http://pubs.acs.org.

■ AUTHOR INFORMATION

Corresponding Author

*E-mail: sshen1@cmu.edu.

Present Address

Department of Mechanical Engineering, Carnegie Mellon University, Pittsburgh, PA 15213, USA.

Author Contributions

J.S., B.L., and S.S. conceived and designed the experiments. J.S. performed the experiments. P.L. and L.Y.N. contributed sample fabrication. S.S., J.S., and B.L. wrote the paper. All authors discussed the results and commented on the manuscript. S.S. supervised the research.

Notes

The authors declare no competing financial interest.

■ ACKNOWLEDGMENTS

We want to thank Matthew Moneck for the assistance on CMP. This work is supported by US National Science Foundation (NSF) grant number CBET-1253692 for near-field thermal measurements and US Defense Advanced Research Projects Agency (DARPA) grant number D14AP00008 for nanowire fabrication.

■ ABBREVIATIONS

HM, hyperbolic metamaterials; PLDOS, photon local density of states; MWAs, metal wire arrays; AFM, atomic force microscope; AAO, anodic aluminum oxide; CMP, chemical mechanical planarization

■ REFERENCES

(1) Otey, C. R.; Lau, W. T.; Fan, S. *Phys. Rev. Lett.* **2010**, *104*, 154301.
(2) Byrnes, S. J.; Blanchard, R.; Capasso, F. *Proc. Natl. Acad. Sci. U.S.A.* **2014**, *111*, 3927−3932.
(3) Padture, N. P.; Gell, M.; Jordan, E. H. *Science* **2002**, *296*, 280−284.
(4) Ben-Abdallah, P.; Biehs, S.-A. *Phys. Rev. Lett.* **2014**, *112*, 044301.
(5) Siegel, R.; Howell, J. *Thermal Radiation Heat Transfer*; Taylor & Francis: London, 2001.
(6) Yu, Z.; Sergeant, N. P.; Skauli, T.; Zhang, G.; Wang, H.; Fan, S. *Nat. Commun.* **2013**, *4*, 1730.
(7) Biehs, S.-A.; Rousseau, E.; Greffet, J.-J. *Phys. Rev. Lett.* **2010**, *105*, 234301.
(8) Messina, R.; Ben-Abdallah, P. *Sci. Rep.* **2013**, *3*, 1383.
(9) Guha, B.; Otey, C.; Poitras, C. B.; Fan, S.; Lipson, M. *Nano Lett.* **2012**, *12*, 4546−4550.
(10) De Wilde, Y.; Formanek, F.; Carminati, R.; Gralak, B.; Lemoine, P.-A.; Joulain, K.; Mulet, J.-P.; Chen, Y.; Greffet, J.-J. *Nature* **2006**, *444*, 740−743.
(11) Challener, W. A.; Peng, C.; Itagi, A. V.; Karns, D.; Peng, W.; Peng, Y.; Yang, X.; Zhu, X.; Gokemeijer, N. J.; Hsia, Y.-T.; Ju, G.; Rottmayer, R. E.; Seigler, M. A.; Gage, E. C. *Nat. Photonics* **2009**, *3*, 220−224.
(12) Poddubny, A.; Iorsh, I.; Belov, P.; Kivshar, Y. *Nat. Photonics* **2013**, *7*, 948−957.
(13) Liu, B.; Shen, S. *Phys. Rev. B* **2013**, *87*, 115403.
(14) Shvets, G.; Trendafilov, S.; Pendry, J.; Sarychev, A. *Phys. Rev. Lett.* **2007**, *99*, 053903.
(15) Joulain, K.; Carminati, R.; Mulet, J.-P.; Greffet, J.-J. *Phys. Rev. B* **2003**, *68*, 245405.
(16) Barnes, J. R.; Stephenson, R. J.; Woodburn, C. N.; O'Shea, S. J.; Welland, M. E.; Rayment, T.; Gimzewski, J. K.; Gerber, C. *Rev. Sci. Instrum.* **1994**, *65*, 3793−3798.
(17) Narayanaswamy, A.; Gu, N. *J. Heat Transfer* **2011**, *133*, 042401.
(18) Shen, S.; Narayanaswamy, A.; Chen, G. *Nano Lett.* **2009**, *9*, 2909−2913.
(19) Rousseau, E.; Siria, A.; Jourdan, G.; Volz, S.; Comin, F.; Chevrier, J.; Greffet, J.-J. *Nat. Photonics* **2009**, *3*, 514−517.
(20) Yao, J.; Wang, Y.; Tsai, K.-T.; Liu, Z.; Yin, X.; Bartal, G.; Stacy, A. M.; Wang, Y.-L.; Zhang, X. *Philos. Trans. A. Math. Phys. Eng. Sci.* **2011**, *369*, 3434−3446.
(21) Nielsch, K.; Müller, F.; Li, A.-P.; Gösele, U. *Adv. Mater.* **2000**, *12*, 582−586.
(22) Chen, R.; Lu, M.-C.; Srinivasan, V.; Wang, Z.; Cho, H. H.; Majumdar, A. *Nano Lett.* **2009**, *9*, 548−553.
(23) Du, T.; Vijayakumar, A.; Sundaram, K. B.; Desai, V. *Microelectron. Eng.* **2004**, *75*, 234−241.
(24) Shi, J.; Li, P.; Liu, B.; Shen, S. *Appl. Phys. Lett.* **2013**, *102*, 183114.

DOI: 10.1021/nl504332t
Nano Lett. 2015, 15, 1217−1221